PAPER Special Section on Emerging Technologies for Practical Ubiquitous and Sensor Networks

Interference-aware Transmission Power Control for Wireless Sensor Networks

Junseok KIM[†*], *Nonmember and* **Younggoo KWON**[†**], *Member*

SUMMARY Maintaining the lowest possible transmission power in the wireless sensor networks (WSNs) is vulnerable to the interference fluctuations because of the bad signal-to-interference-plus-noise-ratio (SINR). The previous transmission power control (TPC) algorithms do not consider much for the interferences from other 2.4GHz devices, which can cause significant performance degradations in real world deployments. This paper proposes the interference-aware transmission power control (I-TPC) algorithm for WSNs. In the proposed algorithm, each node dynamically adjusts the transmission power and the received signal strength (RSS) target, hence the appropriate SINR is provided even when the wireless LAN (WLAN) interferences become strong. The experimental results show that the proposed algorithm outperforms the previous algorithms in terms of the energy and the packet reception ratio (PRR) performance in WLAN interference environments.

key words: *Interference-Aware, Transmission Power Control*

1. Introduction

In the WSNs, the power conservation is very important because nodes are usually operated on limited batteries. A well designed TPC algorithm can reduce the energy consumption and improve the channel capacity. The transmission power should be determined on a link-by-link basis and adapted to wireless channel variations quickly with the minimum overheads [16] [18]. There are many TPC studies in wireless networks [10] [11] [12] [13] [14], which mainly focus on improving the channel capacity. In the WSNs, the energy-efficient network connectivity is studied based on theoretical analysis and simulations [15] [16]. Recently, experimental studies [17] [18] have shown that the TPC reduces the energy consumption in the low-power WSNs. In the transmission power control algorithm with blacklisting (PCBL) [17], each node sends packets at different transmission power levels to determine the optimal transmission power based on the PRR. Lin et al. [18] used the RSS and the link quality indicator (LQI) for radio channel to estimate the optimal transmission power level, and they employ a feedback based adaptive transmission power control (ATPC) algorithm to dynamically adjust the transmission power over time. For the practical implementation of WSNs, we have to consider the effect from various interference sources. Many WSN devices on the market operate on the 2.4GHz ISM band and they are vulnerable to the interferences from other wireless networks such as the IEEE 802.11 WLANs [3] or the IEEE 802.15.1 Bluetooth [5]. Generally, the transmission power of the WSN devices is lower than WLAN or Bluetooth devices. Therefore, the TPC algorithm for WSNs has to consider carefully the interferences from other 2.4GHz wireless devices. Among various interference sources, the interference effect of other 2.4GHz devices can cause significant performance degradation in real world WSN deployments. In this paper, we present a practical TPC algorithm for WSNs, namely, the interference aware transmission power control (I-TPC) algorithm. When other 2.4GHz WLAN devices exist, the SINR at the WSN device can be decreased much below the SINR threshold due to the interference from WLAN devices. In the proposed algorithm, when the interference is detected, each node quickly adjusts the RSS target to provide the acceptable SINR. After that, the TPC is performed based on the determined RSS target for the relatively small variations of link qualities. According to the testbed experimental results, the proposed algorithm provides good PRR performance while reducing much energy consumption even when the WLAN interference is severe. Moreover, in the proposed algorithm, each node can maintain the lowest possible transmission power efficiently with much less overhead.

In the next section, we explain the interference effect on the RSS target. Then, we present the newly proposed algorithm in section 3. The performance evaluations are given in section 4. In the final section, we present the conclusions.

2. Interference Effect on The RSS Target

2.1 Analytical Model

There are three basic parameters which are used to determine the lowest possible transmission power in TPC algorithms: the PRR, the chip correlation indicator (CCI), and the RSS. The PRR is directly related with the link quality, however, the TPC algorithms based on the PRR may cause large overheads and cannot effectively respond to the link quality variations. The CCI

Manuscript received February 22, 2008.
Manuscript revised June 03, 2008.

[†]The authors are with the Department of Electronics Engineering, Konkuk University, 1 Hwayang-dong, Gwangjin-gu, Seoul, 143-701, Korea.
[*]E-mail: jskim@usn.konkuk.ac.kr
[**]E-mail: ygkwon@konkuk.ac.kr

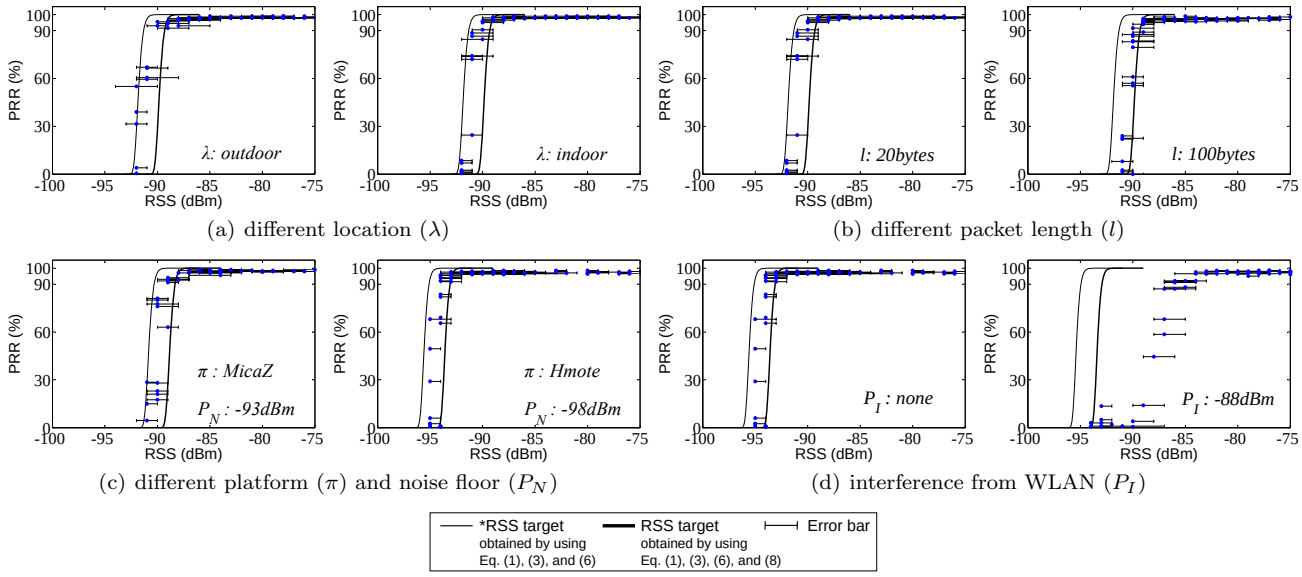

(a) different location (λ) (b) different packet length (l)

(c) different platform (π) and noise floor (P_N) (d) interference from WLAN (P_I)

Fig. 1 RSS vs. PRR under different conditions.

is calculated over the first eight symbols after the start of a packet frame and represents how close the received chip sequences are to the decided symbols [1]. Using the RSS is the most common method to measure the link quality, but there are still controversies [17] [18] [19] [20] [22] [23] because the RSS can be influenced by various environmental factors. However, many previous studies [18] [19] [22] indicated that using the RSS can be an effective approach in TPC algorithms if the proper RSS target, which can satisfy the desired PRR, is provided.

In [22], the PRR can be determined by the bit error ratio (BER) as follows:

$$PRR = (1 - P_B)^{8l} \tag{1}$$

$$P_B = 1 - PRR^{1/8l} \tag{2}$$

where P_B is the BER and l is the frame length of the packet (in bytes). For O-QPSK modulation in the IEEE 802.15.4 standard, P_B is determined as follows [2]:

$$P_B = \frac{8}{15} \cdot \frac{1}{16} \cdot \sum_{k=2}^{16} -1^k \binom{16}{k} e^{20 \cdot SINR \cdot \left(\frac{1}{k} - 1\right)} \tag{3}$$

Using equation (2) and (3), we can obtain the proper SINR target which satisfies the IEEE 802.15.4 receive sensitivity requirement and 99% PRR with 20 bytes packet size as follows:

$$SINR_{target} \approx 0.4021 dBm \tag{4}$$

In [22], the relation between the SINR and the RSS is given by:

$$SINR = 10log \frac{10^{RSS/10} - 10^{P_N/10}}{10^{P_I/10}} \tag{5}$$

where P_N is the noise floor of the receive node in dBm and P_I is the received interference strength in dBm. When we assume that there is no external interference (i.e., $P_I = P_N$), we can derive the analytical RSS target as follows:

$$*RSS_{target} = P_N + 10log\left(10^{\frac{SINR_{target}}{10}} + 1\right) \tag{6}$$

where $*RSS_{target}$ denotes the RSS target determined by the analytical model. Using equation (4) and (6), the analytical RSS target is:

$$*RSS_{target} \approx P_N + 3.216 \tag{7}$$

From the experimental results in [20], there is about 2dB difference between the analytical RSS target and the empirical RSS target. Therefore, we redefine the RSS target as follows:

$$RSS_{target} = *RSS_{target} + 2 \approx P_N + 5.216 \tag{8}$$

We can observe that if the receiver's noise floor is known and there is no interference effect, the proper RSS target can be determined by equation (8) without complex calculation.

2.2 Experimental Studies

To see the various interference effects on the RSS target determination, we conducted several testbed experiments under different conditions. We used Hybus motes [9] and MicaZ [7] motes, and both platforms use the CC2420 radio chip. The Hybus mote is a clone of Tmote Sky [8] and has a 16-bit Texas MSP430F1611 micro controller and an integrated PCB antenna. The MicaZ mote has an 8-bit Atmel ATmega128L micro controller and a detachable monopole antenna. In each experiment, one mote transmits 200 packets at each

transmission power level (range from 3 to 31) and the other mote records the RSS and the PRR values. The packet rate is 1 packet per second and we vary the distance of nodes from 10 to 40 meters.

Figure 1 shows the correlation between the RSS and the PRR under different conditions. The thin line denotes the analytically determined RSS target, $*RSS_{target}$. From the analytical RSS target, the SINR value can be obtained by equation (6) and from the SINR value, the BER value can be obtained by equation (3). Finally, from the BER value, the PRR value can be obtained by equation (1). Thus, $*RSS_{target}$ can be obtained by using equation (1), (3), and (6). The bold line denotes the redefined RSS target, RSS_{target}, compensating for the difference between the analytical values and experimental results by equation (8). Thus, RSS_{target} can be obtained by using equation (1), (3), (6), and (8). The error bars show the standard deviation of the measured RSS values. From the experimental results, we can observe the following features:

- Packets can not be coherently received when the RSS value is below a certain target, otherwise the PRR is close to 100%;
- The RSS target is strongly correlated with the noise floor when there is no interference effect (see Fig. 1-(c)) because the BER is determined by the SINR (see equation (3) and (5));
- The proper RSS target can be derived by the analytical model when the noise floor of the receiver is known and there is no interference effect;
- The WLAN interference affects much to the proper RSS target value as shown in Fig. 1-(d), whereas the effects from the location, the packet length, and the platform can be included to the existing analytical models;
- The RSS target should be adjusted when the interference becomes strong unless the network performance would be significantly degraded.

3. Design of Interference-aware Transmission Power Control (I-TPC)

3.1 Basic Architecture

The proposed algorithm is basically consisted of two functional procedures: the two-tier transmission power control and the RSS target adjustment. Figure 2 shows the operational characteristics and Fig. 3 shows the basic architecture for the proposed algorithm. At first, the proper RSS target, which can satisfies the desired PRR, is determined by equation (8). Based on the RSS target, each node tries to adjust its transmission power to keep the RSS value within the upper and the lower RSS target values by using the two-tier transmission power control procedure. The net effect of this operation is that the proposed algorithm tries to keep the good link qualities quickly when there are small scale link quality variations. When the interference is detected, the RSS target and the transmission power are increased immediately by the RSS target adjustment procedure to provide an appropriate SINR.

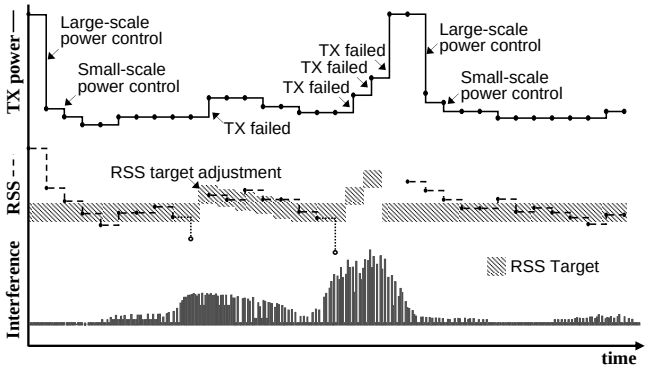

Fig. 2 I-TPC operations.

3.2 Two-tier Transmission Power Control

The two-tier transmission power control procedure is consisted of two phases: the large-scale transmission power control phase and the small-scale transmission power control phase (see Fig. 3). At first, the transmission power is roughly determined through the large-scale transmission power control phase. When a node has a data packet to send, it looks at its neighbor table to find whether the transmission power for the receiver is already determined or not. If the transmission power is not determined, the data packet is sent with the maximum transmission power. When the data packet is received, the receiver returns the RSS value and the noise floor (acquired when the receiver began to run), back through an ACK packet. After the sender received the ACK packet, it determines the proper RSS target for the receiver i, ${}^iRSS_{target}$, by using equation (8). If the noise floor is -96dBm, then, the RSS target is determined as -90dBm (rounded off from -90.787). After that, the sender determines the proper transmission power, ${}^iP_{TX}$, as follows [27]:

$$ {}^iP_{TX} = P_{TX}^{MAX} + \left({}^iRSS_{target} - RSS\right) \quad (9) $$

If ${}^iRSS_{target}$ and RSS are -90dBm and -80dBm, it means that the maximum transmission power is 10dB stronger than the lowest possible transmission power. Thus, the sender reduces the transmission power by 10dB.

$$ {}^iP_{TX} = P_{TX}^{MAX} + \left({}^iRSS_{target} - RSS\right) + M \quad (10) $$

As shown in Fig. 1, the measured RSS value has around 3dB variance on the average. This means that packet transmission can be failed if the transmission power is determined by using the RSS target value only. To

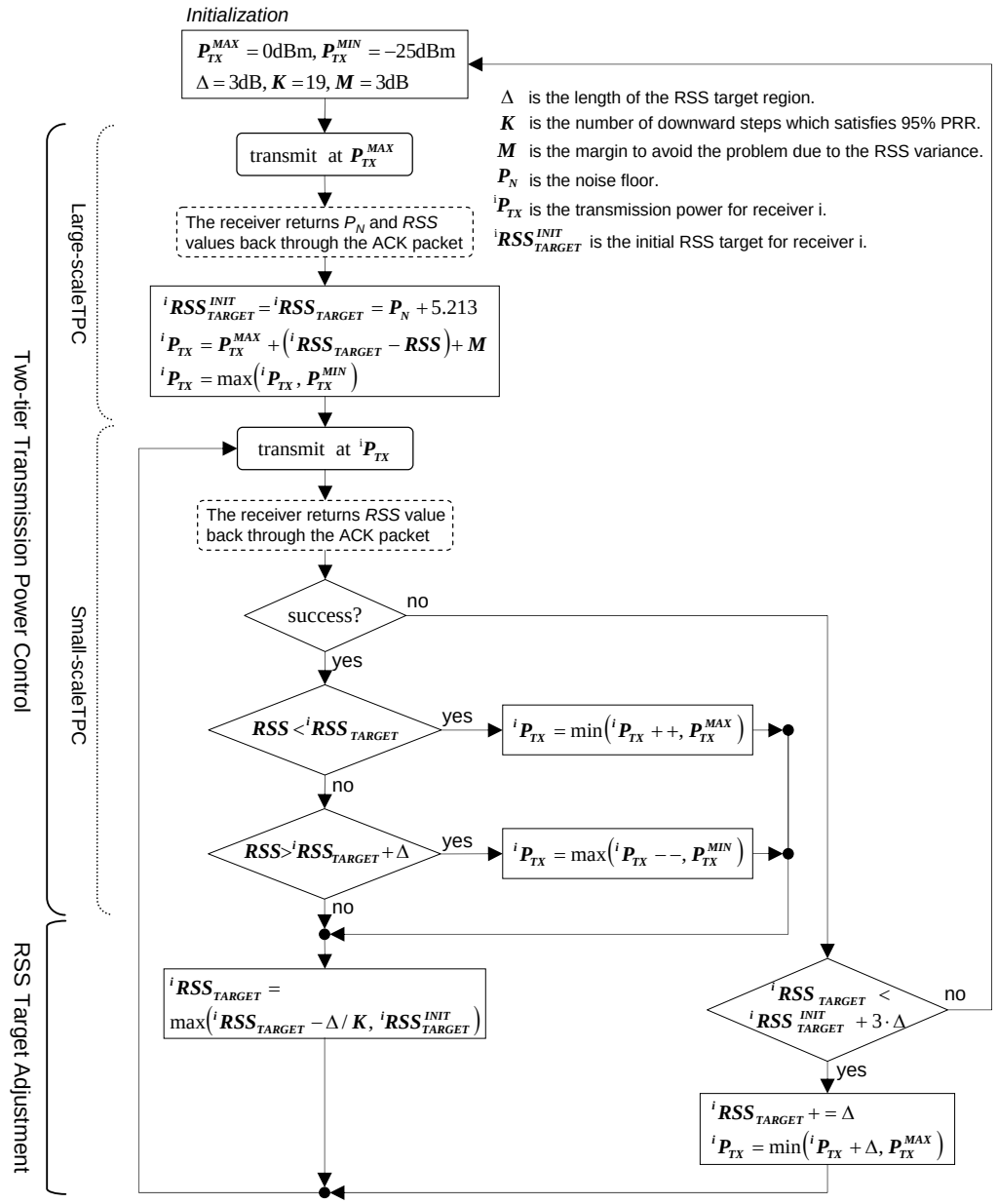

Fig. 3 Basic architecture.

avoid the transmission failure due to the RSS variance, we give a 3dB margin, M.

After the large-scale transmission power control phase, if the sender has data packets to the same receiver, the transmission power is slightly adjusted in the fixed size of 1dB through the small-scale transmission power control phase to keep a good link quality:

- If $RSS < RSS_{target}$: ${}^iP_{TX}$ is increased by 1dB;
- Else if $RSS > RSS_{target} + \Delta$: ${}^iP_{TX}$ is decreased by 1dB.

${}^iRSS_{target}$ and ${}^iRSS_{target}+\Delta$ denote the lower and the upper RSS targets respectively. Δ denotes the length of the RSS target region (see Fig. 4). We set Δ as 3dB because the transmission power difference between nearby levels is 2dB on CC2420 [1]. In the small-scale transmission power control phase, each node tries to maintain the lowest possible transmission power by considering the proper RSS target value.

3.3 RSS Target Adjustment

Based on the experimental results for the interference effects in section 2.2, the RSS target has to be adjusted when the wireless link quality is much unstable or the interference from other 2.4GHz devices becomes strong. As shown in Fig. 4, we set three RSS target regions and define a simple RSS target adjustment rule as follows:

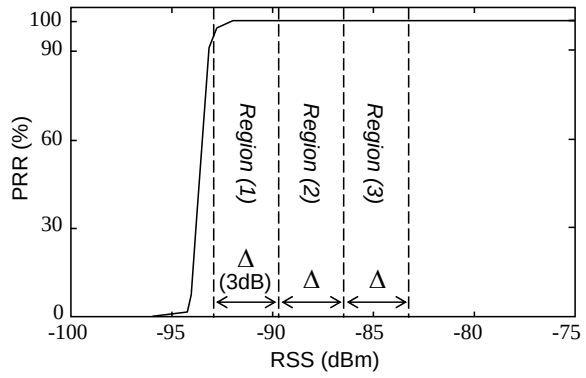

Fig. 4 Three RSS target regions.

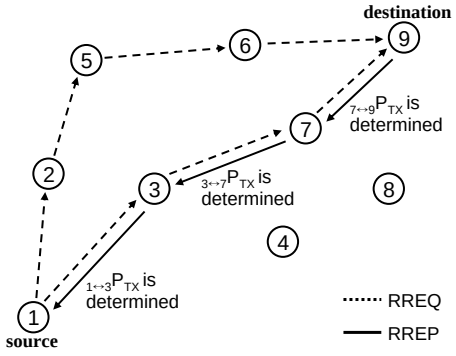

Fig. 5 AODVjr operation.

- If packet in error: RSS_{target} is increased by Δ;
- Else: RSS_{target} is decreased by Δ/K.

When a transmission failure occurs, the RSS target jumps from $Region(j)$ to $Region(j+1)$. When a transmission is successfully completed, the RSS target steps down from $Region(j+1)$ to $Region(j+1)-\Delta/K$ until it reaches the initial RSS target, ${}^{i}RSS_{target}^{init}$. To maintain a steady RSS target on the average, an upward jump is followed by K downward steps. K is related with the desired PRR, PRR_D, as follows [11]:

$$K = \frac{PRR_D}{1 - PRR_D} \tag{11}$$

In our implementation, we set K as 19 to provide 95% PRR. That is, the 3dB increased RSS target is gradually returned to the initial RSS target after 19 consecutive successful transmissions.

In the proposed algorithm, each node can maintain the lowest possible transmission power efficiently with much less overhead. Moreover, the proposed algorithm can effectively handle the interference of other 2.4GHz devices by adjusting the transmission power and the RSS target dynamically.

3.4 Co-operation with Ad Hoc Routing Algorithm

We implemented the proposed algorithm with the AODVjr routing algorithm [29]. The AODVjr is a simplified version of the AODV [28] and is used as a routing algorithm of the ZigBee protocol [4]. In the AODVjr, the route discovery procedure is performed through the route request (RREQ) and the route reply (RREP) message exchanges, as shown in Fig. 5. Because the RREQ message is broadcasted, the RSS value is returned through the RREP message on the forward path. After the route discovery procedure is finished, the transmission powers are dynamically maintained when the on-the-route nodes exchange the data and CONNECT messages. That is, the proposed algorithm is operated when nodes exchange RREQ, RREP, CONNECT, and data messages.

4. Performance Results

We now evaluate the performance of the proposed algorithm and compare it with the PCBL and the ATPC performance results. The testbed device is the Hybus mote [9] which is the clone of Tmote Sky [8].

To evaluate the energy consumption, we analyze the energy consumption parts as follows:

$$\begin{aligned} E &= E_S + E_R \\ E_S &= E_S^{TX} + E_S^{RX} \\ &= P_{TX}^{j} \times T_{DATA} + P_{RX} \times (T_{MAC} + T_{ACK}) \\ E_R &= P_{TX}^{j} \times T_{ACK} + P_{RX} \times (T_{MAC} + T_{DATA}) \\ T_{MAC} &= T_{LIFS} + T_{BO} + T_{SIFS} \end{aligned} \tag{12}$$

where E_S and E_R denote the energy consumptions of the sender and the receiver. P_{TX}^{j} and P_{RX} are the transmission power with the transmission power level of j and the receive power. T_{DATA}, T_{ACK}, T_{LIFS}, T_{SIFS}, and T_{BO} denote the durations of the data packet, the acknowledge packet, the long inter-frame space, the short inter-frame space, and the backoff time respectively [2]. We do not consider the energy consumption for idle listening period.

4.1 Single Hop Scenario with No WLAN Interference

We first investigate the single-hop scenario that there is no interference of 2.4GHz devices. In the experiments, the sender periodically transmits 100 byte data packets to the receiver at a rate of 0.8Hz for one hour by using different power transmission algorithms, and we repeated each experiment 5 times. Table 1 shows that all TPC algorithms consume much less energy than the MAX scheme when the distance is 30 feet. The MAX scheme means that the sender transmits data packets with the maximum transmission power. When the distance is 70 feet, the performance of the PCBL algorithm goes down compared with other TPC algorithms. The proposed algorithm achieved better performance results than the ATPC. The reason is that the transmission

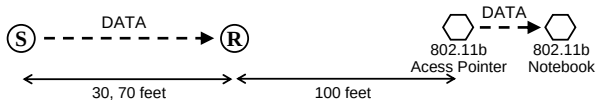

Fig. 6 Single hop scenario.

Table 1 Energy consumption (uJ/Byte) and PRR (%) performance with no WLAN interference.

	MAX	PCBL	ATPC	I-TPC
distance	30 feet			
E_S^{TX}	1.67	**0.87**	**0.89**	**0.86**
E	4.92	**4.18**	**4.18**	**4.14**
PRR	100	**98**	**98.8**	**99.2**
distance	70 feet			
E_S^{TX}	1.68	**1.02**	**1.01**	**1.03**
E	4.96	**4.45**	**4.36**	**4.34**
PRR	99.2	**94.8**	**97.2**	**98.4**

power of the proposed algorithm can be quickly adjusted over time, whereas the transmission power of the ATPC is slowly adjusted by using the feedback mechanism.

4.2 Single Hop Scenario with WLAN Interference

The proposed algorithm is designed to handle the interferences of other 2.4GHz devices. To demonstrate this advantage, we used two WLAN devices in the experiments, which is shown in Fig. 6. In the experiment, there is no significant interference from WLAN devices in the first 30 minutes and the WLAN notebook (SONY VAIO UX27) downloads a big file from a FTP server via the WLAN AP (ipTIME G504) in the last 30 minutes. The frequency channels of the WSN device and the WLAN device are 26 and 13 respectively. We placed an extra mote near the WSN receiver to check the interference of WLAN over time (see Fig. 7).

Table 2 shows that the performance results of the PCBL and the ATPC algorithms are significantly degraded regardless the distance. As shown in Fig. 8, the PCBL and the ATPC algorithms show the good PRR performance above 95% in the first 30 minutes, but the PRR results are rapidly decreased after that. The energy performances of the PCBL and the ATPC are even worse than the MAX because of many packet transmission failures under WLAN interference environments. The PCBL shows the lowest performance because it cannot dynamically adapt the transmission power according to the link quality variations. In the ATPC, the SINR at the receiver is decreased much below than the SINR threshold when the WLAN interference becomes strong because the RSS target is fixed. The proposed algorithm reduces the energy consumption E by 12% compared with the MAX scheme. In addition, the proposed algorithm provides a good PRR performance of 97% even when the WLAN interference is severe.

Table 2 Energy consumption (uJ/Byte) and PRR (%) performance with WLAN interference.

	MAX	PCBL	ATPC	I-TPC
distance	30 feet			
E_S^{TX}	1.67	**1.40**	**1.21**	**1.01**
E	4.92	**6.12**	**5.38**	**4.35**
PRR	100	**68.97**	**77.94**	**97.31**
distance	70 feet			
E_S^{TX}	1.67	**1.55**	**1.33**	**1.07**
E	4.93	**6.68**	**5.68**	**4.43**
PRR	99.68	**63.35**	**74.80**	**97.09**

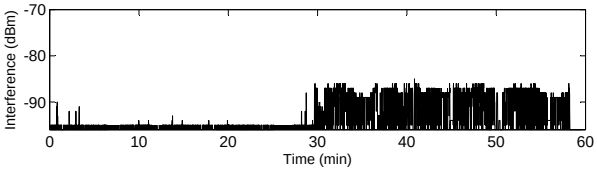

Fig. 7 WLAN interference at WSN receiver.

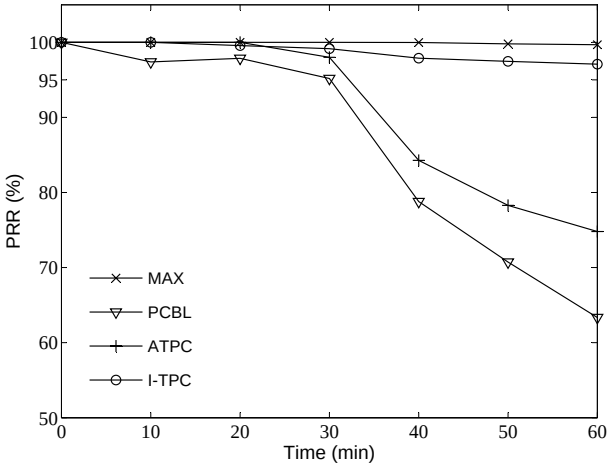

Fig. 8 PRR vs. time with WLAN interference.

4.3 Ad-hoc Network Scenario

Generally, many sensor devices form an ad-hoc network in the real-world deployment. We implemented the proposed algorithm with the AODVjr routing algorithm [29]. At first, we perform the experiment of the ad-hoc network scenario when there is no interference from other 2.4GHz devices (see Fig. 10). The source node (numbered as 1) begins the path discovery procedure by broadcasting the RREQ message, and after the path discovery procedure is finished, it periodically transmits 100 byte data packets at a rate of 0.8Hz for one hour.

Table 3 shows the energy consumption for the path discovery procedure and the initial transmission power determination procedure. In the PCBL algorithm, each node has to transmit a number of packets to determine the transmission power based on the PRR value.

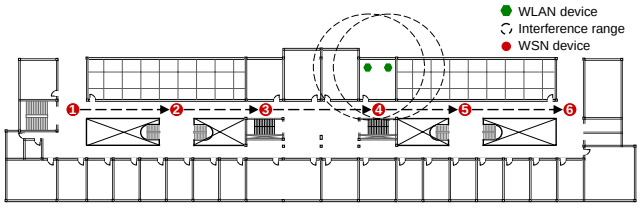

Fig. 9 Ad-hoc network scenario.

Table 3 Energy consumption (mJ) for the path discovery and the initial transmission power determination procedures.

PCBL	ATPC	I-TPC
172.509	**47.833**	**4.504**

Table 4 Energy consumption (uJ/Byte) and PDR (%) performance with no WLAN interference.

	MAX	PCBL	ATPC	I-TPC
E_S^{TX}	8.37	**5.45**	**4.87**	**4.90**
E	24.50	**20.52**	**20.03**	**20.07**
PDR	99.60	**89.35**	**95.17**	**97.21**

In the ATPC algorithm, each node has to broadcast BEACON packets to determine the transmission power from the distribution of RSS values at different transmission power levels. In the PCBL and the ATPC algorithms, the overhead of the initialization procedure is much increased as the number of nodes increases. The proposed algorithm generates much less overheads compared with other TPC algorithms. This is a critical advantage in the real world WSNs deployment.

Table 4 shows the energy consumption except the initialization phase and the packet delivery ratio (PDR) performance results when there is no WLAN interferences. The PDR performance will be the multiplication of the PRR value of each hop. The PCBL shows the lowest PDR performance whereas the proposed algorithm shows good PDR performance. We used two WLAN devices (see Fig. 9) to investigate the effects from the WLAN interferences to the performance results of the TPC algorithms. Table 5 shows the energy consumption except initialization phase and the PDR performance results when there are the WLAN interferences in the last 30 minutes during 1 hour experiment. For the same experiment, the PDR performance versus the number of hops is presented in Fig. 10. The PDR performances of the PCBL and the ATPC are significantly degraded because the link qualities of 3→4 and 4→5 are much affected by the WLAN interferences. The proposed algorithm shows 92.54% PDR and this means that the PRR of each link is 98% on the average. In addition, the proposed algorithm saves the energy consumption E by about 11% compared with the MAX when the WLAN interference is severe.

From the various performance results, we can say that the proposed algorithm is robust to the interferences from other 2.4GHz devices and works efficiently with the routing protocol.

Table 5 Energy consumption (uJ/Byte) and PDR (%) performance with WLAN interference.

	MAX	PCBL	ATPC	I-TPC
E_S^{TX}	8.42	**7.82**	**6.40**	**5.18**
E	24.70	**31.61**	**26.66**	**22.15**
PDR	98.67	**56.59**	**70.57**	**92.54**

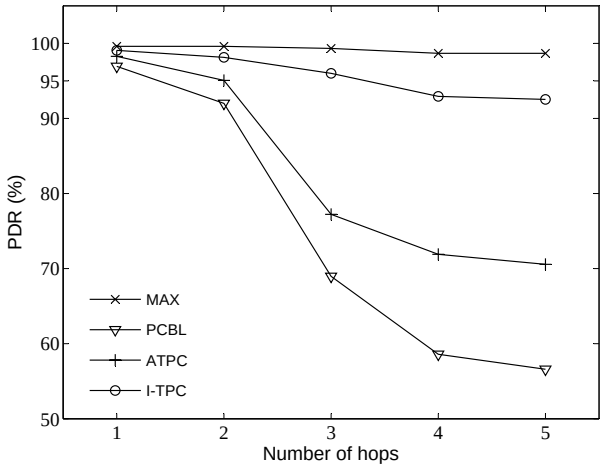

Fig. 10 PDR vs. number of hops with WLAN interference.

4.4 Hidden Node Problem

In CSMA/CA-based MAC, the lowest possible transmission power may enlarge the hidden node problem [24]. To evaluate the performance degradation due to the hidden node problem, we conducted testbed experiments with 3 motes. In each experiment, two senders transmit 50byte data messages continuously to the receiver as shown in Fig. 11. We vary the distance between the receiver and the sender from 10 to 70 feet.

Table 6 shows the PRR performances of the MAX, the I-TPC, and the LOW methods. The LOW method means that the two senders transmit data messages at the lowest possible transmission power. The minimum transmission power is used as the lowest possible transmission power in the 10 feet experiment case. When the distance is 10 feet, the PRR performance of the LOW method is relatively better because each sender is still in the carrier sense range of the other sender. When the distance is 30 and 70 feet, the PRR performances of the LOW method are significantly degraded due to the hidden node problem. In the proposed method, when packet collisions or packet transmission failures are occurred, the RSS target and the transmission power are increased by the RSS target adjustment procedure, thus the hidden node problem can be reduced quickly.

5. Conclusions

This paper presents an interference aware TPC algo-

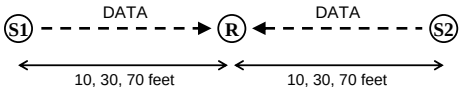

Fig. 11 Congestion scenario.

Table 6 PRR (%) performance under congestion conditions.

distance	MAX	I-TPC	LOW
10ft	96.93	**91.22**	**82.17**
30ft	96.62	**87.43**	**42.86**
70ft	93.40	**82.12**	**41.14**

rithm which provides the power saving characteristic and the high PRR performance simultaneously. The previous TPC algorithms are vulnerable to the WLAN and various types of interferences. In the proposed algorithm, when the interference is detected, each node dynamically adjusts the RSS target value to provide an appropriate SINR. From the various experimental results, we observe that the energy and the PRR performances of the previous algorithms are significantly degraded when the interferences of WLAN devices become strong. The proposed algorithm shows good energy and PRR performances under high level of WLAN interferences, which is one of the most important design issues in the real-world WSN applications.

Acknowledgments

This work was supported by "System IC 2010" project of Ministry of Knowledge Economy.

References

[1] CC2420, "2.4GHz IEEE 802.15.4 / zigbee RF transceiver," http://www.chipcon.com, Nov. 2003.
[2] IEEE Std 802.15.4, "Part 15.4: wireless medium access control (MAC) and physical layer (PHY) specifications for low-rate wireless personal area networks (LR-WPANs)," http://standards.ieee.org/wireless, Oct. 2003.
[3] IEEE Std 802.11, "Wireless LAN medium access control (MAC) and physical layer (PHY) specifications," http://standards.ieee.org/wireless, 1999.
[4] ZigBee, "Zigbee specification," http://www.zigbee.org, Oct. 2007.
[5] Bluetooth, "Specification of the bluetooth system," http://www.bluetooth.org, Feb. 2001.
[6] TinyOS-2.x, "Tinyos programming," http://www.tinyos.net, Oct. 2006.
[7] MicaZ, "MPR-MIB users manual," http://www.xbow.com, Jun. 2007.
[8] Tmote Sky, "Ultra low power IEEE 802.15.4 compliant wireless sensor module," http://www.moteiv.com, Nov. 2006.
[9] Hybus mote, http://www.hybus.net
[10] J. Zander, "Performance of optimum transmitter power control in cellular radio systems," IEEE Transactions on Vehicular Technology, vol. 41, no.1, pp.57-62, Feb. 1992.
[11] A. Sampath, P. Kumar, and J. Holtzman, "On setting reverse link target SIR in a CDMA system," Proc. VTC, Phoenix, USA, pp.929-933, May. 1997.
[12] A. El-Osery and C. Abdallah, "Distributed power control in CDMA cellular systems," IEEE Antennas and Propagation Magazine, vol.42, no.4, pp.152-159, Aug. 2000.
[13] J. P. Monks, V. Bharghavan, W. Mei, and W. Hwu, "A power controlled multiple access protocol for wireless packet networks," Proc. INFOCOM, Anchorage, USA, pp.219-228, Apr. 2001.
[14] I. Ho, and S. Liew, "Impact of power control on performance of IEEE 802.11 wireless networks," IEEE Transactions on Mobile Computing, vol.6, no.11, pp.1245-1258, Nov. 2007.
[15] M. Kubisch, H. Karl, A. Wolisz, L. C. Zhong, and J. Rabaey, "Distributed algorithms for transmission power control in wireless sensor networks," Proc. WCNC, New Orleans, USA, pp.558-563, Mar. 2003.
[16] S. Panichpapiboon, G. Ferrari, and O. Tonguz, "Optimal transmit power in wireless sensor networks," IEEE Transactions on Mobile Computing, vol.5, no.10, pp.1432-1446. Oct. 2006.
[17] D. Son, B. Krishnamachari, and J. Heidemann, "Experimental study of the effects of transmission power control and blacklisting in wireless sensor networks," Proc. SECON, Santa Clara, USA, pp.289-298, Oct. 2004.
[18] S. Lin, J. Zhang, L. Gu, T. He, and J. Stankovic, "ATPC: adaptive transmission power control for wireless sensor networks," In Proc. SenSys, Boulder, USA, pp.223-236, Nov. 2006.
[19] K. Srinivasan and P. Levis, "RSSI is under appreciated," Proc. EmNets, Cambridge, USA, May 2006.
[20] K. Srinivasan, M. Kazandjieva, S. Agarwal, and P. Levis, "The β-factor: improving bimodal wireless network," Stanford University, Technical Report SING-07-01, 2007.
[21] M. Zuniga and B. Krishnamachari, "Analyzing the transitional region in low power wireless links," Proc. SECON, Santa Clara, USA, pp.517-526. Oct. 2004.
[22] D. O'Rourke, S. Fedor, C. Brennan, and M. Collier, "Reception region characterisation using a 2.4GHz direct sequence spread spectrum radio," Proc. EmNets, Cork, Ireland, pp.68-72, Jun. 2007.
[23] J. Zhao and R. Govindan, "Understanding packet delivery performance in dense wireless sensor networks," Proc. Sensys, LA, USA, pp.1-13, Nov, 2003.
[24] Y. Zhou and S. Nettles, "Balancing the hidden and exposed node problems with power control in CSMA/CA-based wireless networks," Proc. WCNC, New Orleans, USA, pp.683-688, Mar. 2005.
[25] J. Jeong, D. Culler, and J. Oh, "Empirical analysis of transmission power control algorithms for wireless sensor networks," Proc. INSS, Braunschweig, Germany, pp.27-34, Jun. 2007.
[26] J. Kim, S. Chang, and Y. Kwon, "ODTPC: on-demand transmission power control for wireless sensor networks," Proc. ICOIN, Pusan, Korea, Jan. 2008.
[27] S. Doshi and Y. Brown, "Minimum energy routing schemes for a wireless ad hoc network," Proc. INFOCOM, New York, USA, pp.212-220, Jul. 2002.
[28] C. Perkins and E. Royer, "Ad-hoc on-demand distance vector routing," Proc. WMCSA, New Orleans, USA, pp.90-100, Feb. 1999.
[29] I. Chakeres and L. Klein-Berndt, "AODVjr, AODV simplified," SIGMOBILE Mobile Computing and Communications Review, vol.6, no.3, pp.100-101, Jul. 2002.
[30] B. A. Zurita, P. G. Park, C. Fischione, A. Speranzon, K. H. Johansson, "On power control for wireless sensor networks: system model, middleware components and experimental evaluation," Proc. ECC, Kos, Greece, Jul. 2007.
[31] A. Woo and D. Culler, "A transmission control scheme for